

Microstructure of AlCrFeSi Alloys Prepared by High-Pressure Spark Plasma Sintering

Anna Knaislová¹, Daniel Kučera¹, Alena Michalcová¹, Ivo Marek¹, Sławomir Cygan², Lucyna Jaworska²

¹Department of Metals and Corrosion Engineering, University of Chemistry and Technology Prague. Technická 5, 166 28 Prague. Czech Republic. E-mail: knaisloa@vscht.cz

²The Institute of Advanced Manufacturing Technology. Wroclawska 37A, 30-011 Krakow. Poland

The rapidly solidified aluminium alloy with slowly diffusing transition metals (iron, chromium) prepared by powder metallurgy techniques is characterized by higher thermal stability in comparison with other common aluminium alloys thanks to hardening of dispersed intermetallic phases. The solubility of transition metals in aluminium is increased by rapid solidification, however, their content, in the alloy, is simultaneously significantly reduced due to the formation of hard and brittle intermetallic phases, which lessen plasticity, ductility, and strength of the material. This work is devoted to the description of a microstructure of AlCr6Fe2Si1 alloy prepared by gas atomization followed by consolidation by High-Pressure Spark Plasma Sintering, and comparison of the influence of various sintering conditions on the microstructure of alloy. The low-porosity compacted alloys are formed by quasi-crystalline phase $\text{Al}_{13}\text{Fe}_4\text{Cr}$, the crystalline phase $\text{Al}_{13}\text{Cr}_2$, and $\text{Al}_{80}\text{Cr}_{13.5}\text{Fe}_{6.5}$ in the aluminium matrix. They are formed by powder particles with the different internal morphology of intermetallic phases (spherical clusters or snowflakes).

Keywords: Gas atomization, Aluminium alloys, X-ray diffraction, Spark Plasma Sintering, Microstructure

1 Introduction

Aluminium and its alloys are widely used materials due to their excellent properties, such as low density, high strength/weight ratio, electrical conductivity or high resistance against corrosion [1-4]. Aluminium alloys are used as construction material for automotive and aerospace industry, especially for their low weight [5]. Aluminium alloys can substitute heavier materials like steel and copper [2, 3]. However, some properties of the alloys are not sufficient for their applications in extreme conditions, such as using at high temperature. For example, the low thermal stability of aluminium precludes its alloy for using as a construction material for internal combustion engines [6].

Increasing of thermal stability can be achieved by alloying elements such as transition metals with a low diffusion coefficient in aluminium [7, 8]. However, these elements such as chromium, iron or nickel have low solubility in aluminium and preparation of these alloys with conventional metallurgical processes do not achieve a desirable result [9].

Al-Fe-Cr alloys are characterized by quasi-crystalline phases surrounded by the α -Al matrix [10]. In previous studies, a strong dependence of the morphology of intermetallic phases on the particle size of the powder of AlCr6Fe2Si1 and AlCr6Fe2Ti1.5Si1 alloys prepared by melt atomization was found. Uniformly distributed spherical intermetallic phases are dominant morphology of small powder particles (in the range of 25-45 μm). Phase formed by irregular star-shaped particles is dominant in larger particle sizes of powder (approximately 100-125 μm). Other less occurring phases are the needle intermetallic phases or colonies of intermetallic phases [11]. Al-Cr-Fe alloy systems are usually formed by Al matrix, $\text{Al}_{13}\text{Cr}_2$ and $\text{Al}_{13}\text{Fe}_4$ phases. Observed quasicrystalline phases in earlier studies of the AlCr6Fe2Si1 system are for example $\text{Al}_{82}\text{Fe}_{18}$, $\text{Al}_{95}\text{Fe}_4\text{Cr}$, or $\text{Al}_{74}\text{Cr}_{20}\text{Si}_6$ [11].

Higher solubility of chromium in aluminium is achieved by rapid solidification methods. The solubility of chromium in aluminium exceeds 6 at. % versus equilibrium solubility, which is 0.2 at. % [11]. Higher thermal resistance can be achieved by the addition of chromium into aluminium, and it is due to the very low diffusion coefficient of chromium in the α -Al matrix. According to Michalcová et al., high thermal resistance correlates with the predominant occurrence of the $\text{Al}_{13}\text{Cr}_2$ phase formed in the triple junction point of the grains of the aluminium matrix [12]. Chromium has also a slow diffusion rate and forms finely dispersed phases, which inhibits grain growth. Chromium in solid solution and as a finely dispersed phase increases the strength of alloys slightly [13]. Refinement of the iron particles from the needles to the small platelets or up to granulated particles can be achieved by the addition of chromium into Al-Si-Fe alloys. This change is probably connected with the chemical change of α -AlFeSi phase to α -Al(Fe,Cr)Si phase [14]. Iron in these alloys forms $\text{Al}_{13}\text{Fe}_4$ phase, which has an impact on coarsening of microstructure at high temperature. Iron does not increase the thermal stability. Present $\text{Al}_{13}\text{Fe}_4$ phase on the grain boundaries increases the diffusion rate of iron in α -Al matrix [12]. Addition of silicon in Al-Cr-Fe-Ti-Si alloy decreases the diffusion rate of chromium and supports curing reaction at high temperature. Silicon increases strength and creep resistance due to the forming of stable silicides [14].

This work deals with the preparation of AlCr6Fe2Si1 alloy by powder metallurgy using rapid solidification and High-Pressure Spark Plasma Sintering. The microstructure of these alloys will be described.

2 Experiment

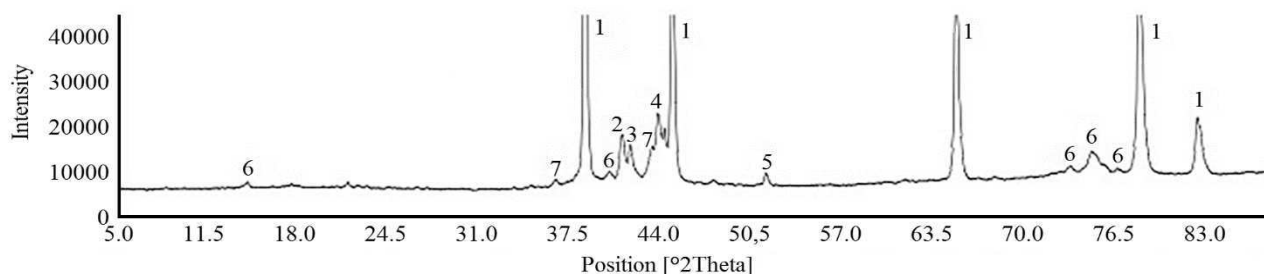
The initial alloy AlCr6Fe2Si1 was prepared by melting high purity aluminium (purity 99.99 %) and pre-alloy AlCr10 (wt. %), AlFe20 (wt. %) and AlSi30 (wt. %) in electric resistance furnace. Thereafter, the alloy was re-

melted in an induction furnace under a nitrogen atmosphere and subsequently atomized by gas atomization. Nitrogen of the pressure 450 kPa was used for melt spraying. Thus prepared powder was then compacted by High-Pressure Spark Plasma Sintering in the Institute of Advanced Manufacturing Technology in Krakow under pressure 6 GPa at 350, 400, 450 and 500 °C for 1 minute.

Metallographic cross-sections of alloys were ground by P80 to P4000 sandpapers (abrasive particles Al_2O_3 and SiC) and polished by Eposil diluted in hydrogen peroxide at a ratio of 1:5 at neoprene disc. After that, the samples were etched by 0.5 % hydrofluoric acid for about 2 seconds. The chemical composition of the powders was detected by X-ray fluorescence ARL 940 XP spectrometer. The microstructure was observed by metallographic microscope Olympus PME3 equipped with the digital camera Carl Zeiss AxioCam ICc3 and AxioVision software. The phase composition was determined using PANalytical X'Pert Pro diffractometer and the HighScore Plus software. The measurement was performed on copper and cobalt lamp. The crystallite (coherently diffracting domains) size was evaluated by the Sherrer's calculator from the diffraction patterns using HighScore Plus software and Equation 1:

$$\text{grain size} = \frac{K \cdot \alpha}{B(\text{size}) \cdot \cos \theta} \quad (1)$$

Where K is a dimensionless shape factor, α is X-ray wavelength, $B(\text{size})$ is a structural extension that is the difference between the total width of integration profile of the unknown sample and the standard, θ is the Bragg angle.



1	2	3	4	5	6	7
α -Al	$\text{Al}_{84.6}\text{Cr}_{15.4}$	$\text{Al}_{95}\text{Fe}_4\text{Cr}$	$\text{Al}_{86}\text{Fe}_{14}$	Ni	Al_5Cr	$\text{Al}_{80}\text{Cr}_{20}$

Fig. 1 X-ray diffraction pattern of $\text{AlCr}_6\text{Fe}_2\text{Si}_1$ powder, measured on a copper X-ray lamp

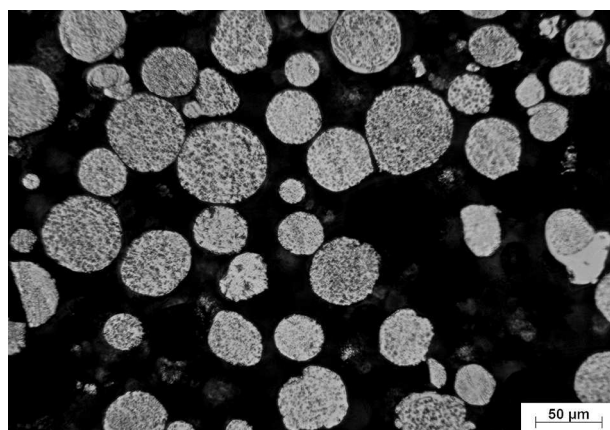


Fig. 2 Morphology of the atomized $\text{AlCr}_6\text{Fe}_2\text{Si}_1$ alloy

The porosity of each sample was measured using the ImageJ program. The average values of at least six measurements are reported in vol. %. Although the porosity was measured on the figures using the software for measuring area representation, it is assumed that the volume fraction shall be equal to the flat rate with the isotropic distribution of pores that can be expected in these alloys [15].

3 Results and discussion

3.1 The initial rapidly solidified powder $\text{AlCr}_6\text{Fe}_2\text{Si}_1$

The chemical composition of the powder detected by X-ray fluorescence is shown in Tab. 1.

Tab. 1 Chemical composition of the initial rapidly solidified powder $\text{AlCr}_6\text{Fe}_2\text{Si}_1$ (wt. %)

Element	Al	Cr	Fe	Si	Ti	Ni
wt. %	85.60	6.69	2.80	1.20	1.58	1.89

Higher amounts of chromium, iron and silicon are a result of the burn off of aluminium due to its reactivity. Impurities of titanium and nickel are likely to get into the powder when the pre-alloys start to melt in the electric resistance furnace. The phase composition of the rapidly solidified powder of $\text{AlCr}_6\text{Fe}_2\text{Si}_1$ alloy was examined by the X-ray diffraction analysis. The results are shown in Fig. 1. The powder is formed by intermetallic phases $\text{Al}_{84.6}\text{Cr}_{15.4}$, $\text{Al}_{95}\text{Fe}_4\text{Cr}$, $\text{Al}_{86}\text{Fe}_{14}$, $\text{Al}_{80}\text{Cr}_{20}$ and Al_5Cr in an aluminium matrix. Elementary nickel is an impurity from the furnace.

Particles of the powder have almost spherical shape, which is typical for gas atomization process. The other particles have an irregular shape caused by particle collisions or imperfections during melting. The microstructure of the powder in cross-section is shown in Fig. 2.

The average grain size of the rapidly solidified alloy is 174 ± 37 nm. Morphology of the intermetallic phases in the powder particles is not always the same, as is shown in Fig. 3a and 3b. Intermetallic phases inside the particles has a typical spherical morphology (Fig. 3a) and sometimes a shape of snowflake or needle (Fig. 3b). Some particles have a distinguished envelope, which was formed by a collision of a solid particle with the melt droplet (Fig. 3a).

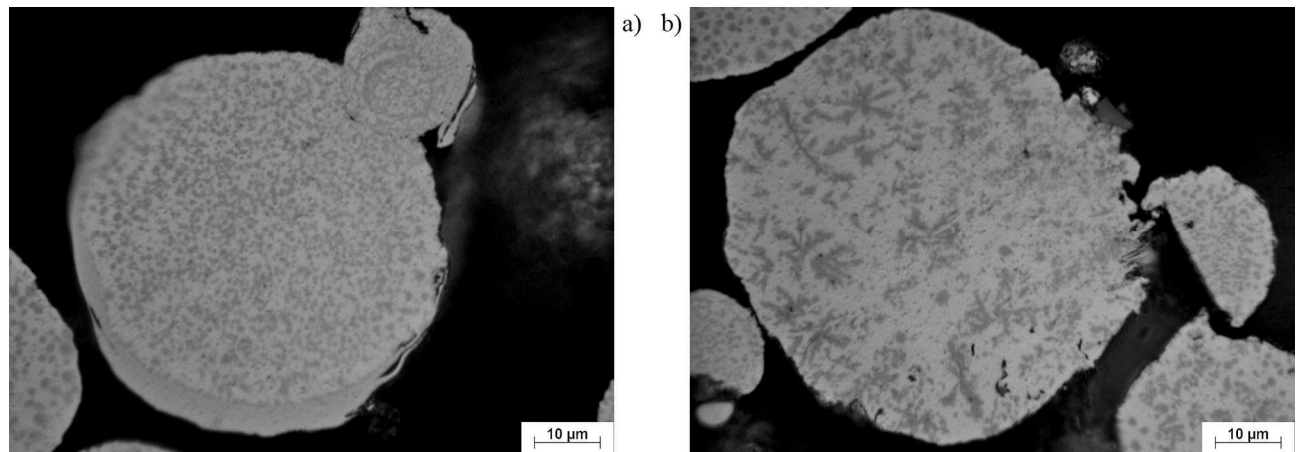


Fig. 3 Cross section of $\text{AlCr}_6\text{Fe}_2\text{Si}_1$ alloy powder particles: a) spherical morphology, b) snowflake, needle morphology

3.2 $\text{AlCr}_6\text{Fe}_2\text{Si}_1$ alloy compacted by High-Pressure Spark Plasma Sintering

The rapidly solidified powder was compacted by High-Pressure Spark Plasma Sintering in the Institute of Advanced Manufacturing Technology in Krakow under pressure 6 GPa at 350, 400, 450 and 500 °C for 1 minute. These four samples have almost the same phase

composition. X-ray diffraction analysis results are shown in Fig. 4. The majority of changes occurs over a range of 44° to 53° on the diffractiopattns, where visible collapses of the metastable phases into are stable phases. The icosahedral quasi-crystalline phase $\text{Al}_{95}\text{Fe}_4\text{Cr}$, the crystalline phases $\text{Al}_{13}\text{Cr}_2$ and $\text{Al}_{80}\text{Cr}_{13.5}\text{Fe}_{6.5}$ in the aluminium matrix were detected by the X-ray diffraction (Fig. 4).

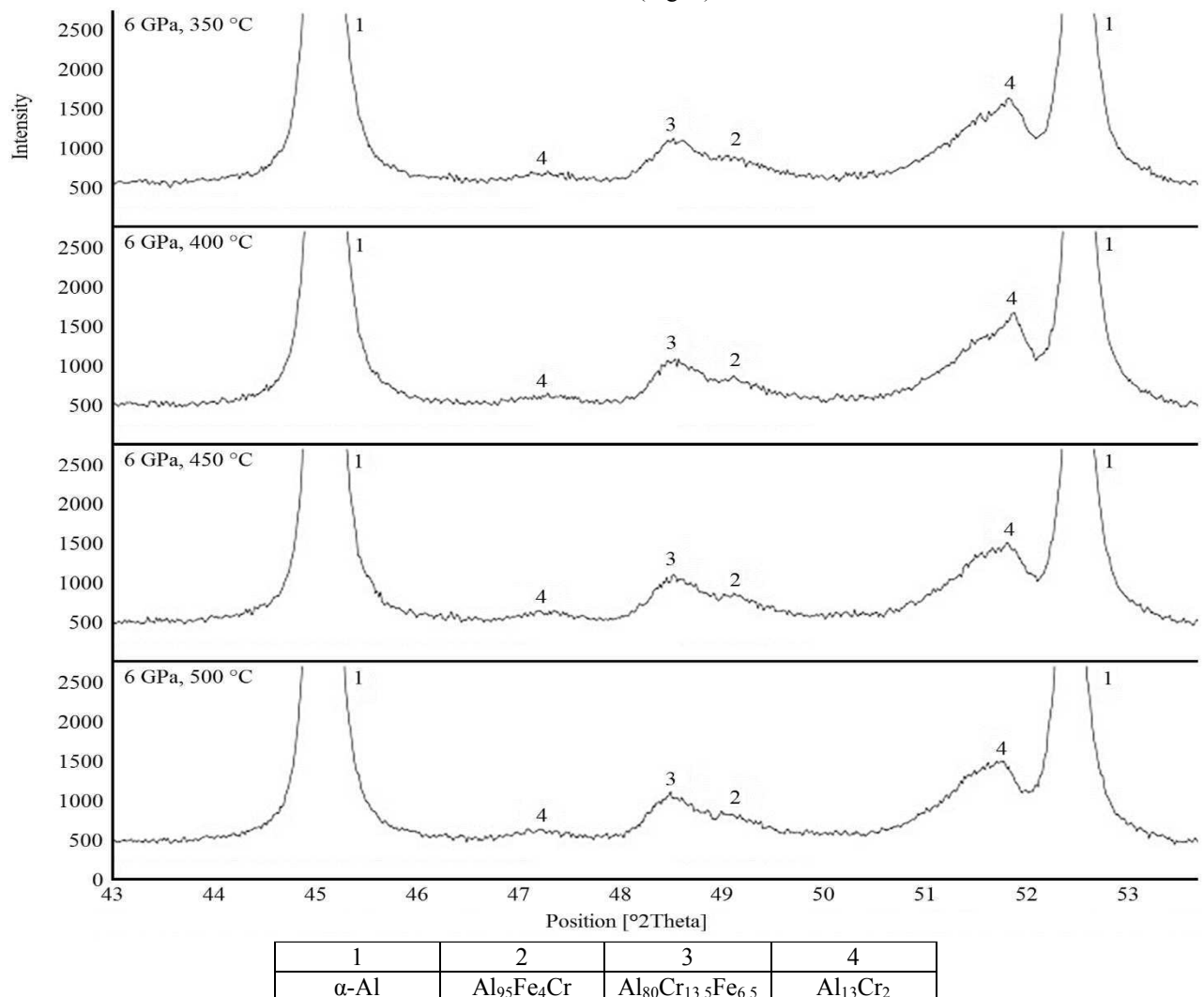


Fig. 4 X-ray diffraction patterns of $\text{AlCr}_6\text{Fe}_2\text{Si}_1$ powder, measured on a copper X-ray lamp

The microstructure of the AlCr6Fe2Si1 alloy prepared by High-Pressure Spark Plasma Sintering is shown in Fig. 5. The structure of all alloys, prepared by different temperatures, is formed by connected particles of powders, the particle boundaries are still visible. The microstructure of alloys is similar and is formed by intermetallic phases with various shapes. The direction of

high-pressure action during SPS process is visible on pictures in Fig. 5, the particles are flattened. The flattening is most visible in the Fig. 5d (HP SPS temperature 500 °C) because higher sintering temperature leads to the easier plastic deformation of particles.

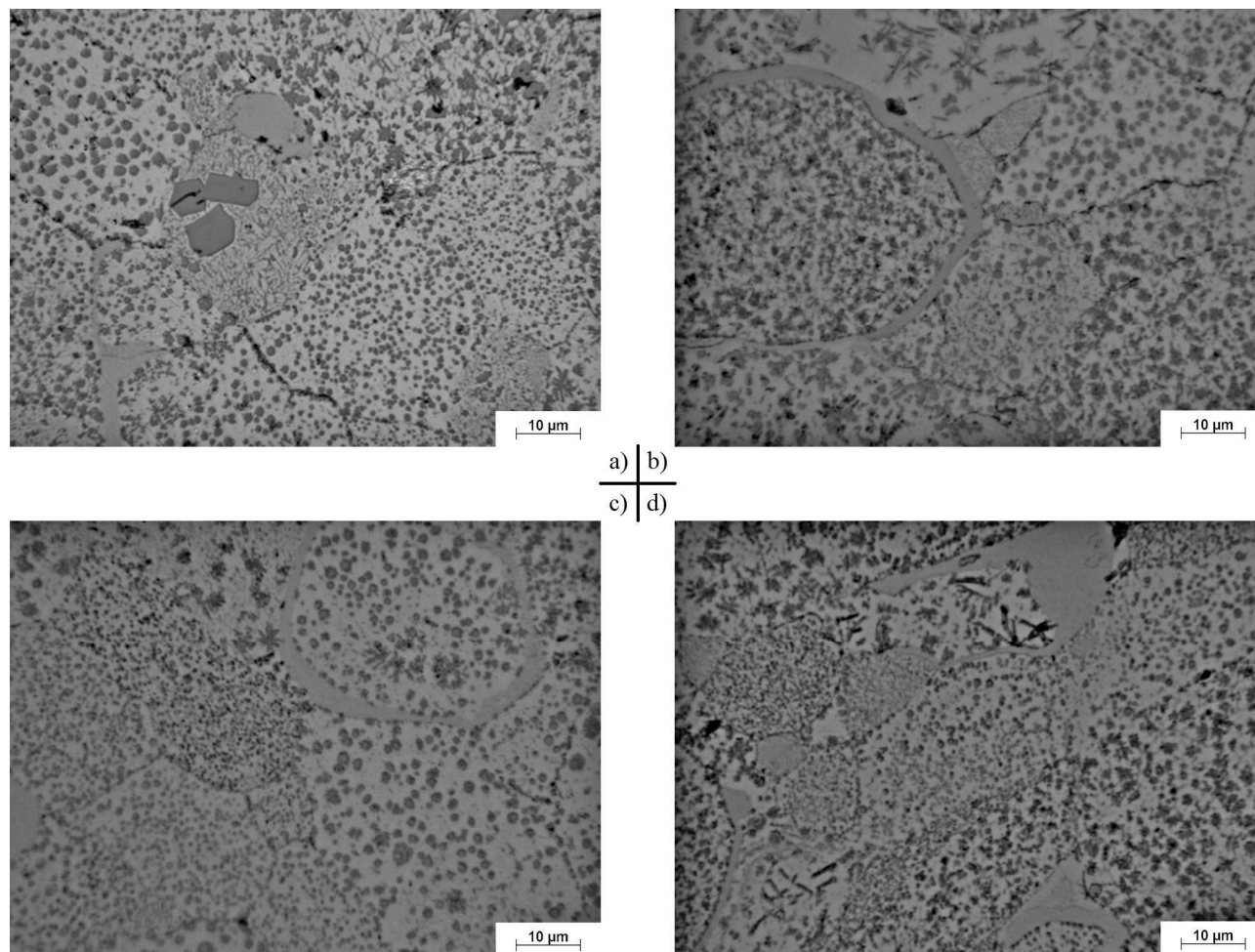


Fig. 5 Microstructure of compacted AlCr6Fe2Si1 alloy prepared by HP SPS a) 350 °C, b) 400 °C, c) 450 °C, d) 500 °C

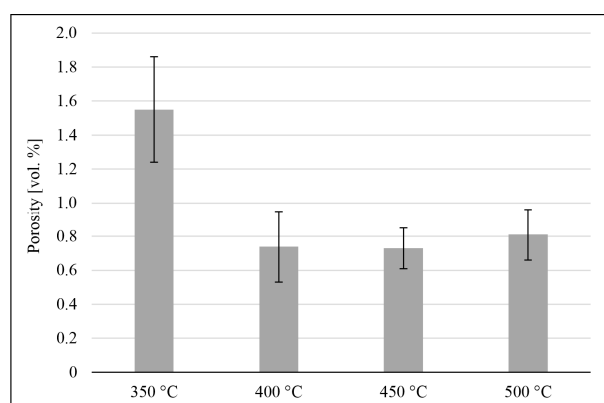


Fig. 6 Porosity of compacted AlCr6Fe2Si1 alloy prepared by HP SPS

AlCr6Fe2Si1 alloy compacted by High-Pressure Spark Plasma Sintering at a temperature of 350 °C has the highest porosity of all alloys. The porosity of this alloy is

1.55 vol. %, the other alloys have a porosity between 0.73 and 0.81 vol. % (Fig. 6). It is due to the easier plastic deformation of material above 400 °C and thereby better consolidation and lower porosity. The grain size of compacted alloys is from 39 to 44 nm, indicating recrystallization during compaction.

4 Conclusion

Rapidly solidified powders of AlCr6Fe2Si1 alloys were compacted by High-Pressure Spark Plasma Sintering. The sintering temperatures were chosen from 350 to 500 °C. All compacted alloys have the same phase composition, but another than the initial powder. Phase transformations of metastable intermetallic phases into more stable phases occurred due to high temperature during sintering. Sintering temperature influenced the microstructure of the samples. The higher sintering temperature was used, the higher deformation of initial powder particles was observed and the lower the

porosity was. Sintering temperature did not influence phase composition of compact samples. Intermetallic phases inside initial powder particles form mostly clusters of spherical or snowflakes shape. The porosity of compacted alloys does not exceed 1.55 vol. %.

Acknowledgement

A.M. and I.M. thank for financial support by Czech Science Foundation, project No. GJ17-25618Y. A.K. thanks for financial support by specific university research MSM No 21-SVV/2018.

References

- [1] VOJTĚCH, D., MICHALCOVÁ, A., PILCH, J., ŠITTNER, P., ŠERÁK, J., NOVÁK, P. (2009). Structural characteristics and thermal stability of Al–5.7Cr–2.5Fe–1.3Ti alloy produced by powder metallurgy. In: *Journal of Alloys and Compounds*, Vol. 475, No. 1, pp. 151-156.
- [2] DENG, W. J., LI, Q., LI, B. L., XIE, Z. C., HE, Y. T., TANG, Y., XIA, W. (2014). Thermal stability of ultrafine grained aluminium alloy prepared by large strain extrusion machining. In: *Materials Science and Technology*, Vol. 30, No. 7, pp. 850-859.
- [3] OÑORO, J., SALVADOR, M. D., CAMBRONERO, L. E. G. (2009). High-temperature mechanical properties of aluminium alloys reinforced with boron carbide particles. In: *Materials Science and Engineering: A*, Vol. 499, No. 1, pp. 421-426.
- [4] NOVÁKOVÁ, I., MORAVEC, J., KEJZLAR, P. (2017). Metallurgy of the Aluminium Alloys for High-Pressure Die Casting In: *Manufacturing Technology*, Vol. 17, No. 5, pp. 804-811.
- [5] PEREIRA, P. H. R., HUANG, Y., LANGDON, T. G. (2017). Examining the Thermal Stability of an Al-Mg-Sc Alloy Processed by High-Pressure Torsion. In: *Materials Research*, Vol. 20, No. 39-45.
- [6] MICHALCOVÁ, A., KNAISLOVÁ, A., MAREK, I., VESELKA, Z., VAVŘÍK, J., BASTL, T., HRDLÍČKA, T., KUČERA, T., LUN, L. L., VOJTĚCH, D. (2017). Powder Metallurgy Prepared Al Alloys and Their „Self-Healing“ Possibilities In: *Manufacturing Technology*, Vol. 17, No. 5, pp. 782-786.
- [7] FROES, F. H., KIM, Y.-W., KRISHNAMURTHY, S. (1989). Rapid solidification of lightweight metal alloys. In: *Materials Science and Engineering: A*, Vol. 117, No. 19-32.
- [8] MICHALCOVÁ, A., VOJTĚCH, D., NOVÁK, P., PROCHÁZKA, I., ČÍŽEK, J., DRAHOKOUPIL, J., WIENEROVÁ, K., SAKSL, K., ROKICKI, P., SPOTZ, Z. (2011). Structure of Rapidly Solidified Al-Fe-Cr-Ce Alloy. In: *Key Engineering Materials*, Vol. 465, No. 199-202.
- [9] VOJTĚCH, D., MICHALCOVÁ, A., PRŮŠA, F., DÁM, K., ŠEDÁ, P. (2012). Properties of the thermally stable Al95Cr3.1Fe1.1Ti0.8 alloy prepared by cold-compression at ultra-high pressure and by hot-extrusion. In: *Materials Characterization*, Vol. 66, No. 83-92.
- [10] GALANO, M., AUDEBERT, F., STONE, I. C., CANTOR, B. (2009). Nanoquasicrystalline Al–Fe–Cr-based alloys. Part I: Phase transformations. In: *Acta Materialia*, Vol. 57, No. 17, pp. 5107-5119.
- [11] BÁRTOVÁ, B., VOJTĚCH, D., VERNER, J., GEMPERLE, A., STUDNÍČKA, V. (2005). Structure and properties of rapidly solidified Al–Cr–Fe–Ti–Si powder alloys. In: *Journal of Alloys and Compounds*, Vol. 387, No. 1, pp. 193-200.
- [12] MICHALCOVÁ, A., VOJTĚCH, D., NOVÁK, P. (2010). Influence of Fe and Cr on properties of rapidly solidified Al-Cr-Fe-Ce alloy. In: *Metal*
- [13] DAVIS, J. R. (2010). *Aluminium and aluminium alloys*. ASM International, Materials Park, OH
- [14] CUI, S., JUNG, I.-H. (2017). Thermodynamic assessments of the Cr-Si and Al-Cr-Si systems. In: *Journal of Alloys and Compounds*, Vol. 708, No. 887-902.
- [15] LINARES-GUERRERO, E. C. (2015). Experimental Study on Inertial Effects in Liquid-Solid Flows. In: *Dissertation (Ph.D.)*